

# Field-testing the Wide-field-of-view Imaging Spectrometer (WFIS)

Robert Haring, Randy Pollock, Richard Cross, Brian Sutin  
Hamilton Sundstrand 2771 North Garey Avenue, Pomona CA 91767

## ABSTRACT

The Wide Field-of-view Imaging Spectrometer (WFIS), a high-performance pushbroom hyperspectral imager designed for atmospheric chemistry and aerosols measurement from an aircraft or satellite, underwent initial field testing in 2004. The results of initial field tests demonstrate the all-reflective instrument's imaging performance and the capabilities of data processing algorithms to render hyperspectral image cubes from the field scans. Further processing results in spectral and photographic imagery suitable for identification, analysis, and discrimination of subjects in the images. The field tests also reveal that the WFIS instrument is suited for other applications, including *in situ* imaging and geological remote sensing.

Keywords: Wide field, imaging spectrometer, hyperspectral, all reflective

## 1. INTRODUCTION

The Wide Field-of-view Imaging Spectrometer, WFIS, is a fast,  $f/2.8$ , all reflective imaging spectrometer with a  $120^\circ$  field of view. Originally intended as a satellite or airborne pushbroom hyperspectral sounder, recent interest has emerged for *in-situ* hyperspectral data acquisition by placing the sensor on a scanning platform. The first WFIS constructed using the patented design<sup>1</sup> was a laboratory demonstrator<sup>2</sup>. This laboratory instrument achieved a spectral resolution ranging from 1 nm to 2 nm over a 500 nm to 1000 nm wavelength range covering a  $70^\circ$  by  $0.08^\circ$  field of view. The WFIS Engineering Model (WFIS EM), pictured in Figure 1, applied the WFIS optical approach to an engineering model suitable for atmospheric chemistry and aerosols measurement from an aircraft or satellite. In this application the instrument operates in the pushbroom-imaging mode. The design of the WFIS EM was funded under NASA's Instrument Incubator Program. A parallel internal IR&D effort at Hamilton Sundstrand Pomona (formerly

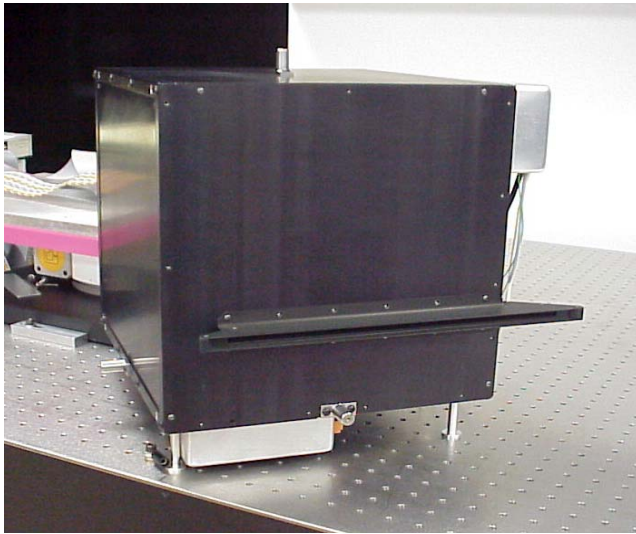
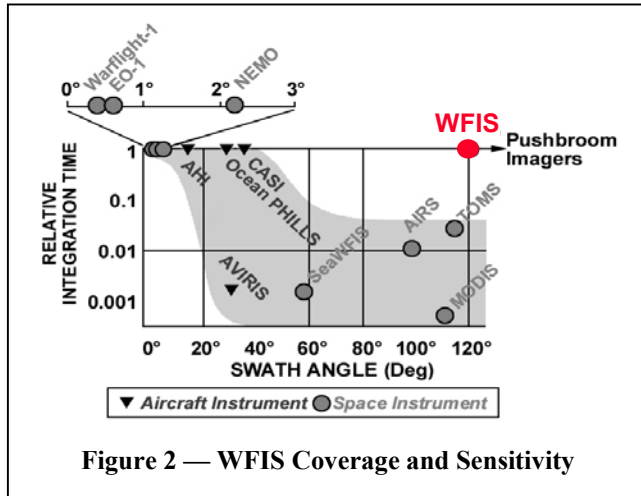


Figure 1 — The Wide Field-of-view Imaging Spectrometer Engineering Model (WFIS EM)

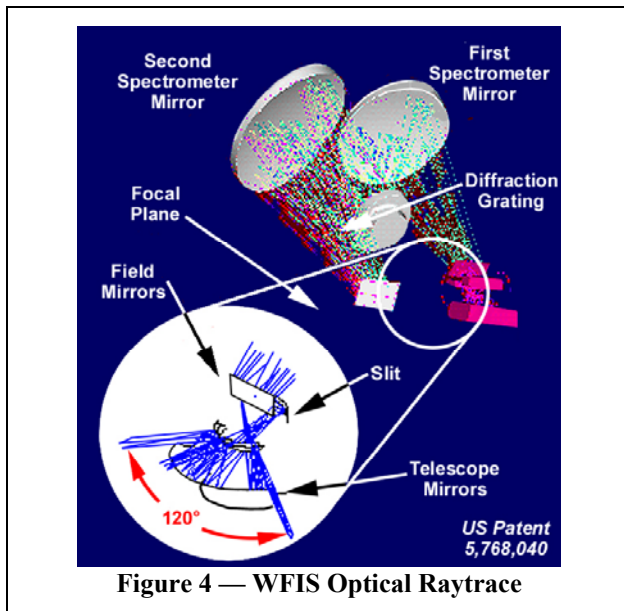
Orbital Sciences Corporation Sensor Systems Division) funded the construction of one engineering model instrument<sup>3</sup>. The results of laboratory tests performed with the engineering model WFIS were presented last year<sup>4</sup>. This paper presents an overview of the Engineering Model (EM) instrument, the field test configuration, the challenges of data handling/processing for a six megapixel hyperspectral sensor, and results of the first field demonstration of the sensor.



desired region. Figure 3, adapted from modified figure originating from Warren J. Smith's *Modern Optical Design* shows the unique solution provided by WFIS. The dark shaded optical design spaces are reflective while the light shaded spaces are refractive. WFIS offers a very wide field of view and fast optical speed in a region currently without an all-reflective solution.

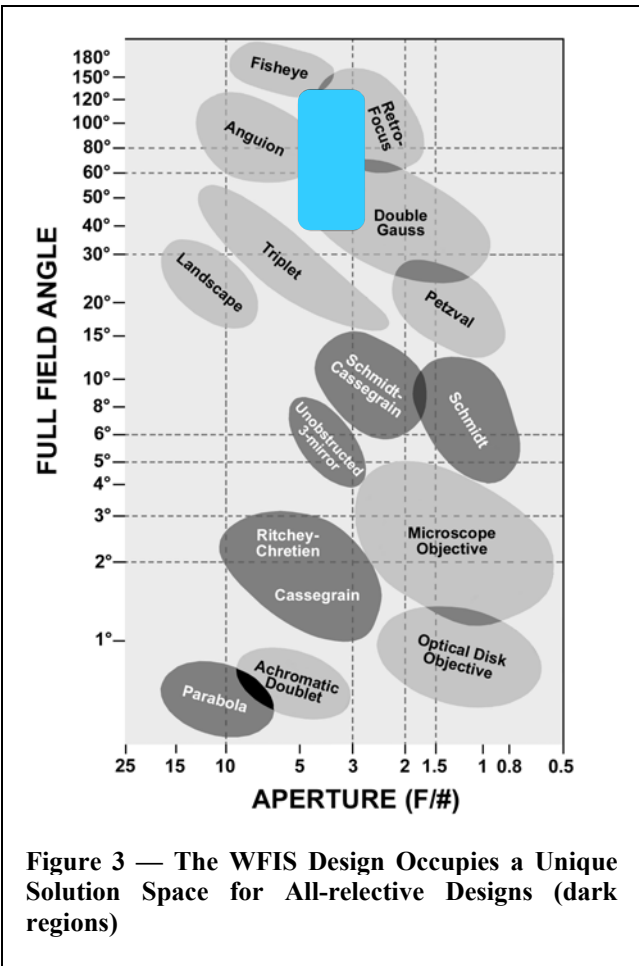
### 1.2. Optical design overview

The WFIS optical design couples an unobstructed Schwartzchild telescope to a three-mirror spectrometer using a unique field mirror arrangement. The field mirrors are off-axis aspheric toroidal elements that flatten the highly curved image of the scene formed by the telescope. An order-sorting filter is necessary at the focal plane to separate overlapping orders. Figure 4 shows a perspective view of the optical path and details of the telescope/field mirror arrangement.



### 1.1. Engineering Model instrument overview

The engineering model WFIS is characterized by its speed,  $f/2.8$ ; wide field of view,  $120^\circ$ ; high spectral resolution,  $1\text{nm}$  to  $1.2\text{ nm}$ ; and wavelength range,  $360\text{ nm}$  to  $1000\text{ nm}$ . This performance can be had without a scanning mechanism. This feature points to a major advantage of the push broom staring design, namely that the entire cross track field is observed continuously. Figure 2 compares the relative integration time with other well know multi-spectral and hyperspectral sensors. The WFIS EM instrument does include a mechanical shutter for the detector; a suitable frame transfer device was not available at the time of its construction. Because of its all-reflective design, WFIS can be adapted to virtually any wavelength region simply by selecting the detector, grating and mirror coatings with those suitable in the desired region.



## 2. ENGINEERING MODEL PERFORMANCE

The WFIS EM design was based on requirements established for an atmospheric science mission. However, the technology can be applied to geological remote sensing either from an aircraft, a space platform, or terrestrial / planetary *in-situ* hyperspectral measurements. The latter requires a scanning platform to provide the scanning motion normally supplied by the forward motion of an aircraft or spacecraft (push broom imaging mode). The commercial CCD in the instrument is a blue enhanced silicon type (un-buffered Kodak front illuminated CCD) requiring a shutter. At this writing an electronically buffered detector slated for installation in the EM is in house to replace the Kodak device and eliminate the need for the mechanical shutter. Table 1 lists requirements for both the atmospheric science and geology applications along side the measured performance of the WFIS EM instrument.

**Table 1 — WFIS Performance versus Requirements**

Parameter	Requirements: Atmospheric Science	Requirements: Geology	WFIS EM Performance
Field of View (Daily Global Coverage from LEO)	≥ 90°	≥ 90°	120°
Angular Resolution, Cross Track, (1 km GSD)	7 mrad	7 mrad	3.49 mrad
Field of View, Along Track (1 km GSD)	7 mrad	7 mrad	3.49 mrad
Integration Time (1 km GSD)	143 ms	143 ms	200 ms, note 2
Spectral Resolution, FWHM	≤ 1 nm	≤ 20 nm	> 0.87 nm
Spectral Sampling	< 0.5 nm	7 nm	0.29 nm
Spectral Range	360 to 1000 nm	0.4 to 10 μm	378 to 1073 nm, note 1
Stray Light	<0.5%	<0.5%	<0.1%
Polarization Sensitivity	<5%	<5%	<5%
Signal to Noise Ratio	> 400	> 100	200, note 2
Wavelength Stability	≤ 0.005 nm	0.5 nm	0.5 nm, note 3
Wavelength Accuracy	≤ 0.02 nm	1 nm	1.0 nm, note 3

note 1: Determined by response of Silicon CCD Focal Plane; all-reflective optics do not constrain spectral range.

note 2: At 700 nm; radiometric performance limited by COTS CCD part selection and operation.

note 3: Estimated; limited by thermal expansion in COTS focal plane PCB and socket.

## 3. FIELD TEST CONFIGURATION

We designed and fabricated the WFIS Engineering Model to operate in field environments for terrestrial and airborne measurements. The first tests scheduled were for terrestrial scans at our facility in Pomona, California. These tests took place in May and June of 2004.

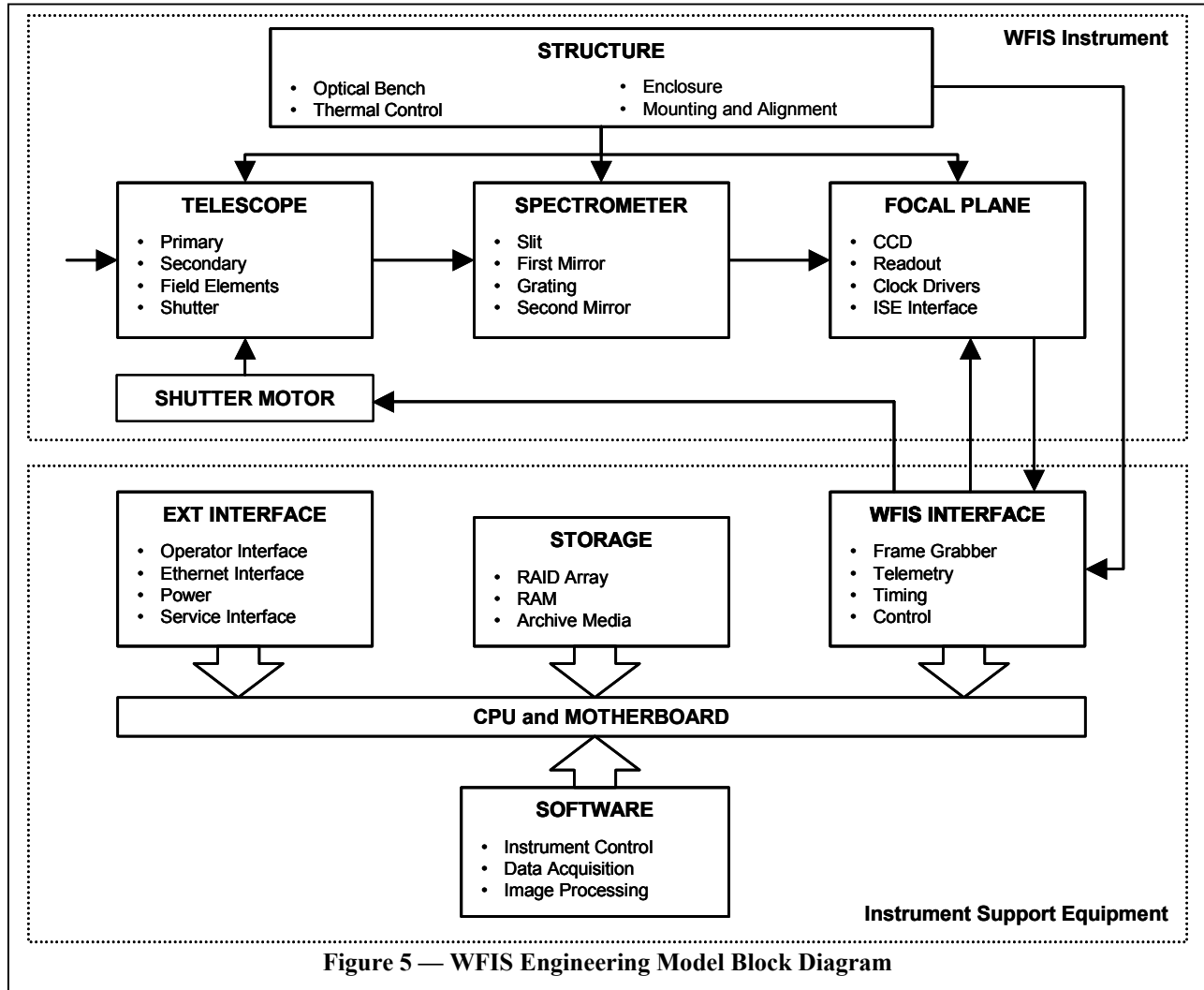
### *Initial Field Test Goals*

Goals for the initial Field Tests were to demonstrate the hyperspectral imaging capability of WFIS, and find the practical limitations of spectral resolution, spatial resolution, and spectral stability. An effective field test would present the instrument with a variety of targets with a range of spectral features, including some with subtle differences, and some with distinctive spectral profiles. Also desired were spatial resolution targets, and targets with interesting and/or aesthetic visual features.

This demonstration was also intended to support a proof of concept hyperspectral imager. The instrument in this application would have a 50° vertical field of view, and be capable of full 360° panoramic imaging with 0.15° spatial sampling in both directions and a 700 nanometer spectral sampling in the MWIR band, using design elements based on the WFIS IR&D efforts. We chose field test parameters that would demonstrate that our protoflight engineering model easily met or exceeded the performance requirements needed for the concept to work.

*Field Test Instrument Setup*

For the initial field test, we oriented the WFIS Engineering Model instrument in an azimuthal scan orientation on an Aerotech rotary stage. The rotary stage fixture supports the three possible orientations of the instruments 120° field of view with respect to the stage axis: azimuthal scan, circumzenith, and coplanar; in a pushbroom imaging aircraft or spacecraft operation, the resulting rotations correspond respectively to pitch, yaw, and roll. Figure 5 is a block diagram depicting the measurement system, including both the instrument and data acquisition system details.



The WFIS Engineering Model electronics consist of a Kodak CCD Evaluation board and a shutter motor driver board. The former is configured to free run, with external switches to configure the integration time. Readout time is 1.2 seconds for the entire array at a pixel read rate of 5 million samples per second, and readouts are digitized to 12 bits. This data is captured by the Data Acquisition system using a Roadrunner frame grabber, and saved to disk with a unique file ID for each frame. Recording to disk is performed in real time using the Video Savant real-time video-processing suite. A Visual C++ executive control program and operator interface allows entry of test conditions and notes, and records this information in an Access database record for each frame.

The free run configuration of the system results in recording only one out of every 2.6 frames collected. This dropout rate has been well characterized, and is quite repeatable over integration times that are much less than the readout period. The phenomenon is partly due to speed limitations of the data acquisition system processor and bus, and is accounted for when configuring the rotary stage scan rates. A computer upgrade will eliminate this inconvenience.

### *Field Test Scene Setup and Operations*

For our first field test scene, we chose our inner courtyard at the Pomona facility. This courtyard encompasses a grassy hill with a stand of Liquid Amber trees, brick and concrete construction, a rose garden, a picnic area, and a wide border covered in ivy. These natural features were supplemented with artificial spatial and spectral targets: a spectralon reference diffuser, an enlarged spatial resolution target, and an inkjet printout of a photograph of the same area of brick wall to be imaged during the test. The WFIS Engineering Model was set up in a shaded area at the southwest corner of the courtyard. We chose June 2, 2004 for our first panoramic test, a day with cloudless conditions in order to avoid sudden variations in illumination during collections.

For a typical collection, initial images are gathered in a static configuration and then analyzed using Video Savant in order to establish the necessary integration time. For field tests, a spectralon reference diffuser is placed in the field of view as a bright reference. Initial dark frames are then collected at the selected integration time with the shutter closed and the entrance baffles shaded and covered with opaque tape. A stage rotation rate is also calculated to provide the desired along-track spatial sampling. Image collections are then initiated with the rotary stage operating continuously at the selected step rate.

For the initial field test scene, an optimal integration time of 200 ms was selected, and 64 dark frames were collected at this configuration. The 1.2 second readout period combined with the integration time resulted in a free run frame rate of 0.714 Hz. Compensating for lost frames, a rotary stage scan rate of 0.412 degrees per second was used; for our 15,000 count per degree encoder, this worked out to 618 encoder counts per second. Our goal was to collect a 120° total azimuth swath, therefore it was necessary to collect at least 800 frames in order to achieve the 0.15° along track spatial sampling desired for this demonstration. To allow some margin for dropout variations and stage operation, we collected 900 frames over a total duration of 58.5 minutes. Following image collection, another series of 64 dark frames were collected. This data was then archived and transmitted to an analysis workstation for further processing.

## **4. DATA COLLECTION AND PROCESSING**

### *Field Test Data Collected*

Field operations on June 2 resulted in a total of 1028 frames collected: 128 dark frames and 900 image frames. Each frame is stored in a 16-bit unsigned TIFF format, each occupying 12.8 Megabytes of data, resulting in a total of over 13 GB of information for a 120° swath. Thus, raw data for a single full circular panorama collected at 0.15° sampling would occupy over 34 GB. The sheer volume of data generated by WFIS EM presents many challenges, not the least of which are data archiving and portability. For real applications, the selection of an appropriate focal plane format to balance sampling performance with data volume will be necessary. For laboratory testing, we chose the largest format CCD available, the six megapixel Kodak KAF-6303. WFIS EM will be refitted with a slightly smaller format frame transfer device prior to more extensive field tests.

### *Field Test Data Processing*

The reduction of raw data into useful image and spectral information entails three main steps: 1) correction for limitations of the instrument and data system, 2) aggregation of individual frames into spectral image sets (hypercubes), and 3) extracting subsets of information from the hypercube to create useful imagery or spectra. Level 0 processing is performed entirely using IDL scripts in batch processing mode, while Level 1 and 2 processing employs ENVI in both script and interactive modes, with final cosmetic work using Excel or GIMP.

## Level 0 Processing

Each raw frame from the WFIS instrument represents an image of the slit dispersed across the focal plane by the diffraction grating. At the image plane, the CCD subtends 3200 pixels across the spatial dimension and 2100 pixels across the spectral dispersion direction. Of these, only an area of 2048 by 2048 pixels is useful information. Some pixels lie outside of the field of view as defined by the instrument's field stops. Other pixels within the field of view see

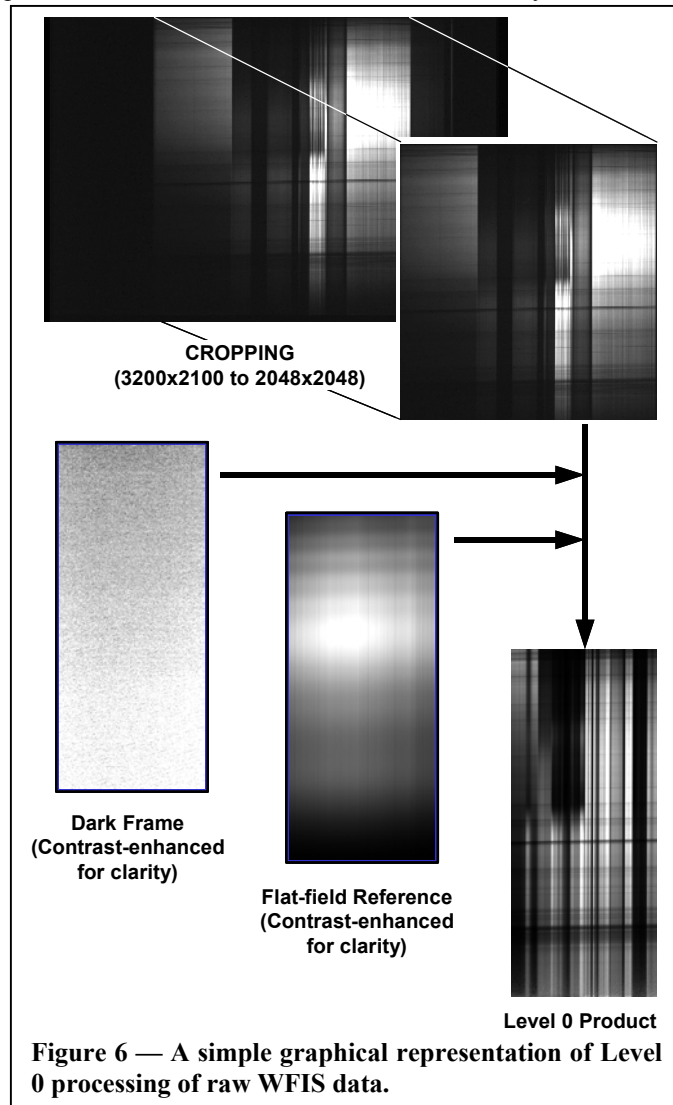


**Figure 6 — A simple graphical representation of Level 0 processing of raw WFIS data.**

only wavelengths for which the CCD has little or no quantum efficiency. These useless pixels are discarded in the first processing step, for all frames, after correcting for any registration errors caused by loss of synchronization between the readout electronics and the frame grabber. To approximate the 50° cross-track FOV requirement of the field test, the spatial field of view was further cropped to 854 pixels. Figure 6 shows actual raw and partially processed frames in a graphical flow representation of Level 0 processing.

Once the raw frames are cropped, rebinning in the spectral or spatial directions is performed to match the data products' spectral and spatial sampling with the imagery requirements. In the case of the initial WFIS Field Tests, 0.15° spatial sampling was achieved by 3x spatial pixel aggregation and 7 nm spectral sampling was achieved by 24x spectral pixel aggregation. Cropping and rebinning the raw data reduces the volume of data by two orders of magnitude, making subsequent numeric processing much easier and more rapid.

The next processing step corrects for fixed pattern nonuniformities in pixel sensitivity and dark response. Dark offset correction is performed by subtraction of the average value of 128 frames collected under dark conditions. Flat-field correction is accomplished by dividing by the normalized value of multiple uniformly illuminated frames collected during laboratory characterization of WFIS. These values are also scaled by the integration time used to collect the imagery in order to obtain an approximate radiance value.

Finally, a statistical resampling of the resulting calibrated frames is performed to correct for residual smile and keystone errors. The WFIS EM exhibits a very slight but measurable smile, and a small clocking misalignment of the grating with respect to the slit imparts a slight nonorthogonality between the spatial axis and the spectral dispersion. This nonorthogonality is modeled as a keystone error for numerical resampling.

## Level 1 Processing

The result of Level 0 processing is a data set representing the desired hypercube at the desired resolution. However, the individual TIFF files represent spectral vs. spatial slices of individual azimuth stations along the swath imaged. We desire a complete hypercube data structure, optionally with individual image files representing the entire panoramic scene generated for each spectral sample.

For this transformation, we employ the interactive and batch script features offered by Research Systems' ENVI software. Spectral "slices" are generated successively from corresponding rows of individual level 0 processed frames, and a BIL hypercube is accumulated incrementally. The hypercube can then be mirrored and rotated as necessary to provide an accurate photographic representation of the imaged scene. Figure 7 is an individual spectral "slice" for the 917 nanometer band, generated from the June 2, 2004 field test.

## Level 2 Processing

The resulting hypercube incorporates far too much data to display in a convenient human-friendly manner, so additional processing is necessary to present data from which results and conclusions can be drawn. WFIS Hyperspectral data cubes are the basis for Level 2 data products such as false color images, synthetic multispectral data sets, point spectra for subjects of opportunity within the image, and orthogonal projections of the hypercube into a 2-dimensional image format.

For the WFIS Field Test, three kinds of level 2 products were generated, all using standard ENVI features: hypercube projections, synthetic band resampling, and point spectra. Point spectra were acquired using ENVI Z-profile features and exported to MS Excel for graphic representation.

## **5. RESULTS**

### *Hypercube Projection and Synthetic Color Image*

Figure 8 is an annotated 2D projection of the 3D hypercube. The front face is a RGB color resampling using the Landsat Thematic Mapper visible band profiles. The false-color spectral faces represent low-intensity blue to high-intensity red and saturated white.

### *Opportunity Targets and Point Spectra*

Looking at images of Figure 8, it is not obvious at first glance that there is a complete, full resolution spectrum for each pixel in the image. One can select a target of interest, a particular flora or geological feature, and examine its spectra independent of the rest of the image. The availability of detailed spectra across the entire image permits discrimination and analysis of opportunistic subjects in the scene.

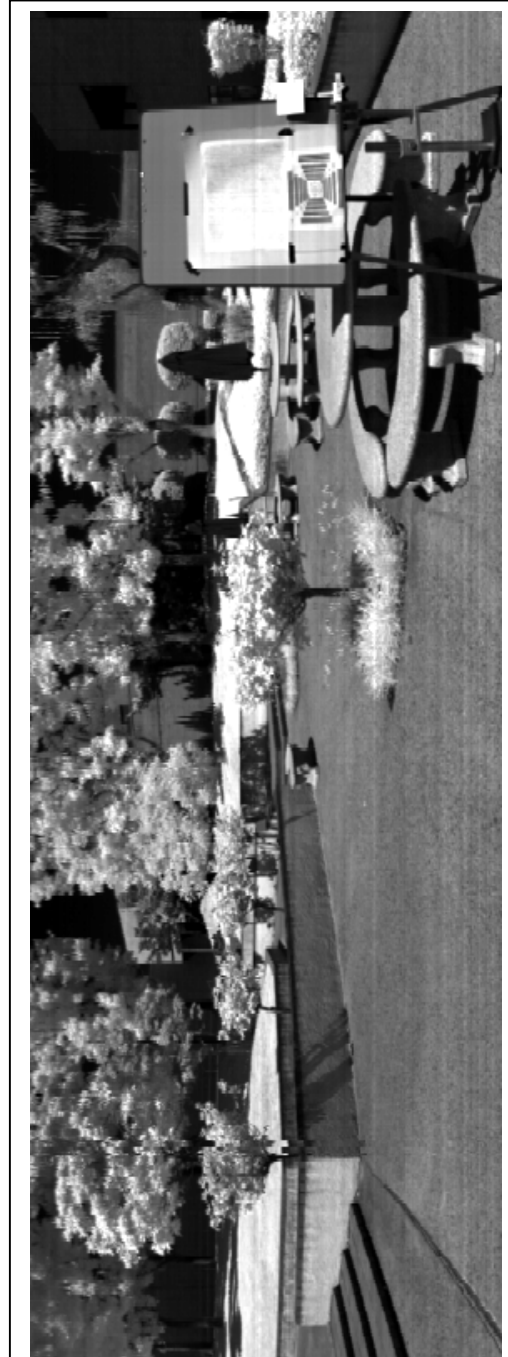


**Figure 7 – Individual Spectral "Slice" Generated for 917 nm by Level 1 Processing**

Figure 9 represents point radiance spectra for three selected pixels in the panorama: Blue sky in the upper right, Red Brick near right center, and a rose leaf in the image center. The visible spectral features are what one would expect: the blue peak in the sky spectrum, the green peak for the foliage, and the prominent red radiance plateau of the bricks. The most noticeable feature of the graph is the infrared spectra of the rose leaf. The prominent NIR radiance peak is a feature of nearly all plants, due to the approximately cubic cellulose structure on a scale of approximately 1 nm that serves as an efficient retroreflector. The distinct absorption feature in this region is the O<sub>2</sub> A-band at 0.76 μm. Another absorption region near 0.95 μm belongs to atmospheric water vapor.

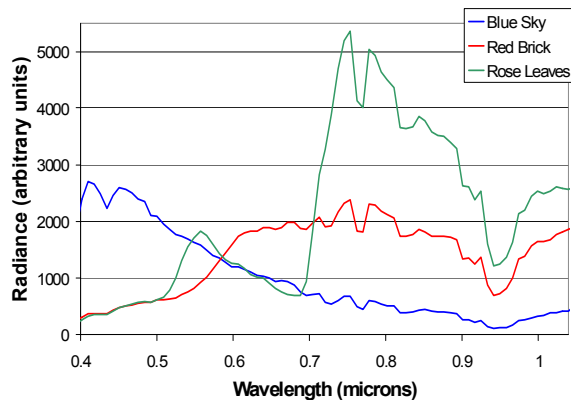
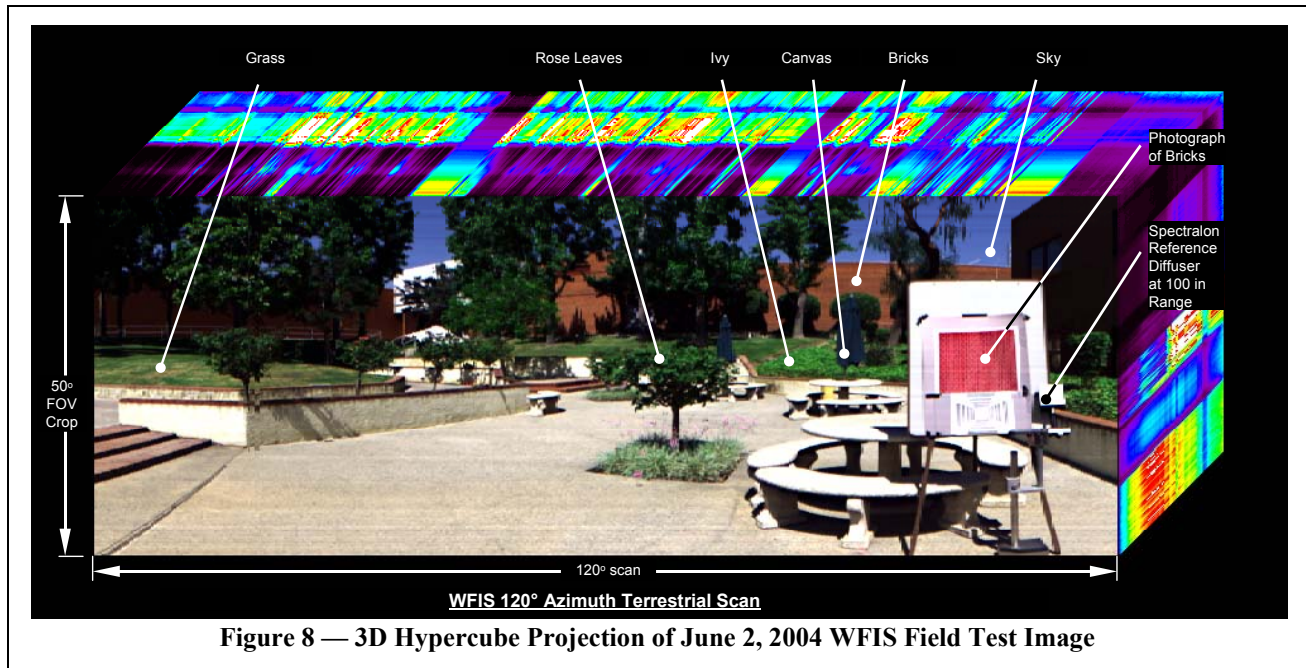


**Figure 9 — Radiance Spectra of Selected Targets**

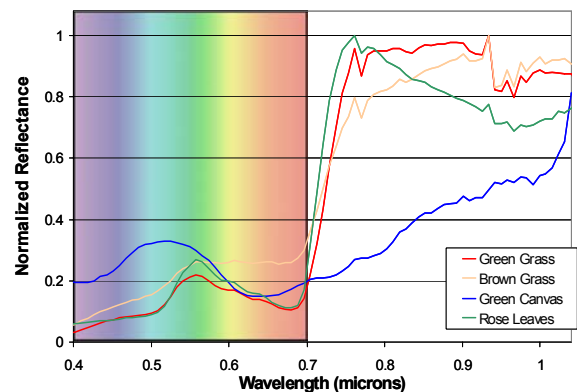


**Figure 10 — Reflectance Spectra of Four Targets**

### *Reflectance Spectra and Target Discrimination*

By including a spectrally flat reference target, it is possible to easily approximate reflectance spectra of selected targets across the image. However, spectral calibration changes during collection will introduce errors in the reflectance curves. Examples of target reflectance spectra and errors appear in Figure 10.

Spectral calibration shifts are most obvious near the A-band absorption features for targets that are separated azimuthally from the reference diffuser. A calibration shift altering the spectral registration of the absorption peaks in the target and reference spectra produce an artifact in the differenced reflection spectrum for the target. Changes in atmospheric path length, registration errors in the raw data, and temperature changes during the course of data collection can all contribute to this error.

Still, conclusions can be drawn from information available at scales larger than the registration error. For instance, the shape of the reflectance spectra can discriminate between foliage species, and even the localized condition of grass of the same variety. Dye peaks in the visible make for easy distinction of green canvas from green foliage. It is already clear that with improved calibration techniques, WFIS will provide the basis for a class of uniquely powerful analytical remote sensing instruments.

## 6. CONCLUSIONS

### *Image Quality and Performance Evaluation*

Laboratory testing<sup>5</sup> confirms that WFIS meets the quantitative requirements established prior to design under laboratory conditions. Many of these performance parameters — such as spectral and spatial sampling and field-of-view — are not subject to change upon introduction to the field. Testing and analysis of the field test data is continuing in order to evaluate the spectral stability performance of WFIS in field conditions. It is already obvious, however, that shortcomings of specific elements are limiting WFIS performance. However, the qualitative performance of the engineering model is remarkable. The first impressions made by WFIS image quality and spectral performances are already proving important to the marketability of this state-of-the-art wide field-of-view high spectral resolution imager.

### *Future Efforts*

We have identified three areas for further development: performance improvements, calibration and data processing techniques, and field test capabilities.

The materials and features of the focal plane and instrument electronics currently limit instrument performance. We plan to replace the full-frame CCD with a frame transfer device, eliminating the shutter and shutter electronics. The readout and control electronics will also be replaced with components more suitable for real-time data acquisition. And a final alignment of the grating to eliminate spectral/spatial nonorthogonality at the image plane is required.

A new calibration fixture will eliminate residual fixed pattern noise present in the flat field reference frame. The current flat field illumination fixture only subtends 7° of the instrument field of view. A new fixture in production will extend this to the full 120° field. Procurement of a faster data acquisition system will enable faster scan speeds and eliminate registration problems.

The operability of the instrument under field test conditions can be improved significantly. Techniques and equipment for improved outdoor operations are easily addressed with existing commercial equipment. These improvements include: purge ports for positive pressure contamination control in the field; more compact and portable power supplies and peripherals; dedicated shipping containers; and improvements to the operator software allowing real time image previews generated during scans.

## REFERENCES

1. S. Macenka, G. Hartmann, R. Haring, H. Roeder, "Wide Filed-of-View Imaging Spectrometer," US Patent No. 5,768,040 (1998)
2. R. Haring, F. Williams, G. Vanstone, G. Putnam, "WFIS: A Wide Field-of-View Imaging Spectrometer," in *Infrared Spaceborne Remote Sensing VII*, Proc. SPIE 3759 (1999)
3. R. E. Haring, G. Vanstone, F. Nguyen, C. Rodil, "Optomechanical design of the incubator Wide Field-of-View Imaging Spectrometer," in *Current Developments in Lens Design and Optical Systems Engineering*, Proc. SPIE 4093, (2000)
4. R. Haring, R. Pollock, and R. Cross, "A Wide Field-of-view Imaging Spectrometer (WFIS), From Laboratory Demonstration to Fully Functioning Engineering Model," in *Infrared Spaceborne Remote Sensing IX*, Proc. SPIE 4486 (2001)
5. R. Haring, R. Pollock, and R. Cross, "Wide Field-of-view Imaging Spectrometer (WFIS) Engineering Model Laboratory Tests and Field Demonstration," in *Infrared Spaceborne Remote Sensing XI*, Proc. SPIE 5152 (2003)